scientific reports

Check for updates

OPEN

Study of biochar in cementitious materials for developing green concrete composites

Ravi Patel[1], Jarvis Stobbs[2] & Bishnu Acharya[1]✉

Biochar is a waste biomass derived carbon enriched solid material that is capable for carbon sequestration. This study illustrates a revolutionary study on the waste biomass pyrolyzed biochar-based concrete with 0–5 wt% cement replacement by the biochar as a potential binder material without using any petroleum-derived superplasticizer. The mechanical strength properties along with the water absorption of the proposed hybrid composite are evaluated for a fixed concrete composition. Moreover, the volumetric property of the formed concrete is determined using the synchrotron-based micro-computed tomography. This study revealed that biochar incorporation up to optimum concentration helps in enhancing the mechanical strength properties of concrete. The optimum dosage of biochar which is 2 wt% increases the compressive strength, splitting tensile strength, and flexural load at fracture by 18.95%, 19.64%, and 12% respectively. Moreover, the optimum sample has shown lowest water absorption among all other samples which indicated reduced porosity in the concrete with biochar introduction. X-ray diffraction analysis confirmed the more production of calcium-silicate-hydrate hydration products for the optimum biochar-augmented concrete composites which resulted in high strength concrete formation. However, the higher concentration of biochar seemed to have negative influence on the strength and durability properties of the concrete which can be seen in terms of physical strength properties and water absorption data. Nonetheless, our novel design of biochar-based concrete can open up a new field of biochar application in construction materials without sacrificing its mechanical strength and water absorption properties to develop green concrete composites.

Keywords Solid waste management, Engineered Biochar, Physical strength properties, Carbon sequestration, Green concrete composites

Concrete is a crucial and inseparable part of modern civilization to build reliable and long-lasting domestic and commercial structures. It provides structural durability, strength, and versatility during the construction process along with providing robust, affordable, and abundantly available options for new development. Concrete is generally composed of cement, sand, gravel, and water, in which cement being the major constituent of concrete mixture. However, concrete usually has different compositions based on the final application of the material. The cement is mainly made up of tri-calcium silicates (C_3S), di-calcium silicates (C_2S), tri-calcium aluminates, and tetra-calcium aluminoferrites in 50–70%, 15–30%, 5–10%, and 5–15% respectively[1]. These are the important constituents (mainly di- and tri- calcium silicates) of cement that take part in hydration reaction to help calcium hydroxide, and calcium-silicate-hydrate (C-S-H) gel formation as described in the reaction (1)[1]. However, several other trace compounds are also present including potassium and sodium oxides, and gypsum which accounts for less than 5%[2].

$$2\ (CaO)_3\,(SiO_2)\ +\ 7H_2O\ \rightarrow\ 3\ Ca\,(OH)_2 +\ (CaO)_3\,(SiO_2)_2\,4\,(H_2O) \tag{1}$$

According to Statistica (2023), the global cement production was estimated to be 4.1 billion tons in 2022, approximately 195% more than that was in 1995 which shows huge reliance on cement for construction materials. However, the cement production is one of the largest carbon dioxides (CO_2) emitter industrial sector worldwide, which contributes around 7% that includes production, preparation, and processing phases[3]. The limestone calcination process is the major bottleneck for CO_2 production directly to the environment which

[1]Department of Chemical and Biological Engineering, University of Saskatchewan, 57 Campus Drive, Saskatoon, SK S7N5A9, Canada. [2]Canadian Light Source, 44 Innovation Boulevard, Saskatoon, SK S7N2V3, Canada. ✉email: bishnu.acharya@usask.ca

happens around 1000^0C. The cement contributes only 20% of the total volume of the concrete but accounts 90% for the total CO_2 emission[4]. That necessitated research for alternative supplementary materials to partially or fully replace cement to reduce the carbon footprint and make the concrete production process greener and more sustainable. Various supplementary cementitious materials have been investigated to mitigate the direct CO_2 emission to the environment and strengthen the concrete properties mainly are ground granulated blast furnace slag (GGBS)[5–8] silica fume (SF)[9–11] pulverized fly ash (PFA)[12–15] metakaolin (MK)[16,17] glass[18–22]copper slag[23–25] waste eggshells[26–30] lignin[31,32] and tires and rubber[33–36] etc. The utilization of these materials serves double benefit, firstly, it mitigates the carbon dioxide emission by reducing the actual quantity of cement used in the concrete, and secondly, by diverting industrial waste materials from directly going to landfills, and to achieve sustainability. For instance, the partial replacement of eggshell powder in the range of 5, 10, and 15 wt% of cement using two fineness (50 and 100 micron), revealed that 10 wt% replacement with 50-micron fineness have higher compressive strength compared to the controlled sample with 10% be the optimum replacement[37]. Islam and co-workers studied the waste glass powder in 0–25 wt% replacement of cement and mortar and found that recycled glass concrete and mortar showed better compressive strength compared to the control samples[21]. In another study, the mixture of glass powder and silica fume were used to partially replace cement in the concrete mixture[38]. He discovered that by using the mixture of glass powder and silica fume increases compressive strength, tensile strength, and flexural strength up to 8.64, 15, and 7.08% respectively after 28 days of curing upon 30% replacement.

There is a growing interest in the utilization of waste biomass products in construction materials to enhance the physical properties of conventional concrete for effective waste management practices and to reduce the carbon footprint of the cement used. Primarily, the waste biomass residues were directly incinerated in open fields to avoid the handling cost or landfill which produces methane gas a more potent greenhouse gas. Certain natural fibers like bamboo, flax, cotton, hemp, jute, hardwood or softwood are a strong natural fiber source[39–43] and bio-based additives like cellulose nanocrystals[44–46]lignin[31,47] that is readily available and cheap source to develop reinforced concrete. However, preprocessing is required to directly use those fibers into concrete matrix and that adds more cost to the process. Moreover, the hydrophilic properties of natural fibers adversely affect the durability (especially water absorption) of the resultant fiber reinforced concrete composite. As a solution, these organic waste materials can be pyrolyzed to biochar, which is a carbon rich highly porous solid material derived from thermochemical conversion of lignocellulosic biomass in the limited/controlled oxygen environment in the temperature range of 450-550^0 C[48]. Until this decade, biochar was mainly used as a soil amending or conditioning agent to reduce soil acidity, nutrient leaching, emission of greenhouse gases, fertilizer, and irrigation requirement, and to improve water quality, but now biochar finds its applications in cosmetics, carbon storage, textiles, wastewater treatment, catalysis, polymer composites, and construction materials[49,50]. A very limited study has been carried out to investigate biochar in construction material and carbon sequestration point of view. The highly porous structure and water holding capacity of biochar can be positively used as a "water-pockets" for uniform and timely curing of concrete. The released water can be used for boosting the cement hydration reaction to produce more hydrated products which give ultimate strength to the concrete composites[31]. Moreover, finely pulverized biochar also provides filling effects to reduce the overall porosity to form more dense structure and positively influence its final strength. Biochar also offers advantageous characteristics in reducing the total cement quantity used and subsequently lowers the carbon footprints developed by the production of cement. However, several factors significantly impact the yield, specific surface area, pore volume, and other microstructural properties of the biochar obtained. For instance, biochar produced at low temperature (< 500°C) is most likely to retain its pristine nutrients and organic matter from the source biomass and offers higher biochar yield with less energy-intensive input[51]. These nutrients (Si, and Ca-based compounds) could be helpful to alter the course of the hydration kinetics of the clinker phases[52]. The lower temperature pyrolysis produces more micropores compared to the higher temperature pyrolysis could be advantageous to reduce the overall porosity of concrete by providing filling[53]. Hence, the biomass pyrolyzing conditions should be meticulously considered to obtain desired biochar properties.

This novel research aims to investigate low temperature pyrolyzed waste softwood biochar to partially replace the cement in construction materials. Most of the previous research either focuses on mortar or cement paste wherein this study aims to utilize concrete with fine and coarse aggregated to introduce biochar into the concrete structure. The detailed characterization is carried out for the biochar-based concrete to understand the alteration in properties of hybrid concrete by incorporation bio-based additives. This developed novel biochar-concrete composite is tested for destructive and non-destructive characteristics and to determine the optimal dosage of biochar which can be incorporated without sacrificing its mechanical strength properties. It's noteworthy to mention that this novel research does not use any petroleum-based superplasticizers to adjust the flowability properties of concrete.

Materials and methods

General Use (GU) Portland cement (PC) (Commercial grade Type 10) was obtained from Rona Garden, Saskatoon, Canada. Other materials including sand (fine aggregate) and gravel (coarse aggregate) were also brought from the same source. The coarse aggregates selected in this study were less than 20 mm to minimize uncertainty in strength caused by shape and size. The particle size distribution of cement, sand, and biochar used is shown in Fig. 1. The biochar (SA) used in this study was provided by Titan Clean Energy Projects, Craik, Saskatchewan, Canada (Picture available in Supplementary file S1). It's noteworthy to mention that the biochar was tested as per ASTM C40-04 to check the organic impurities present in the biochar and the results suggested that biochar is free from toxic impurities and can be used in the construction materials application. The brief discussion of the method along with the results are mentioned in the supplementary file S1. The ultimate and

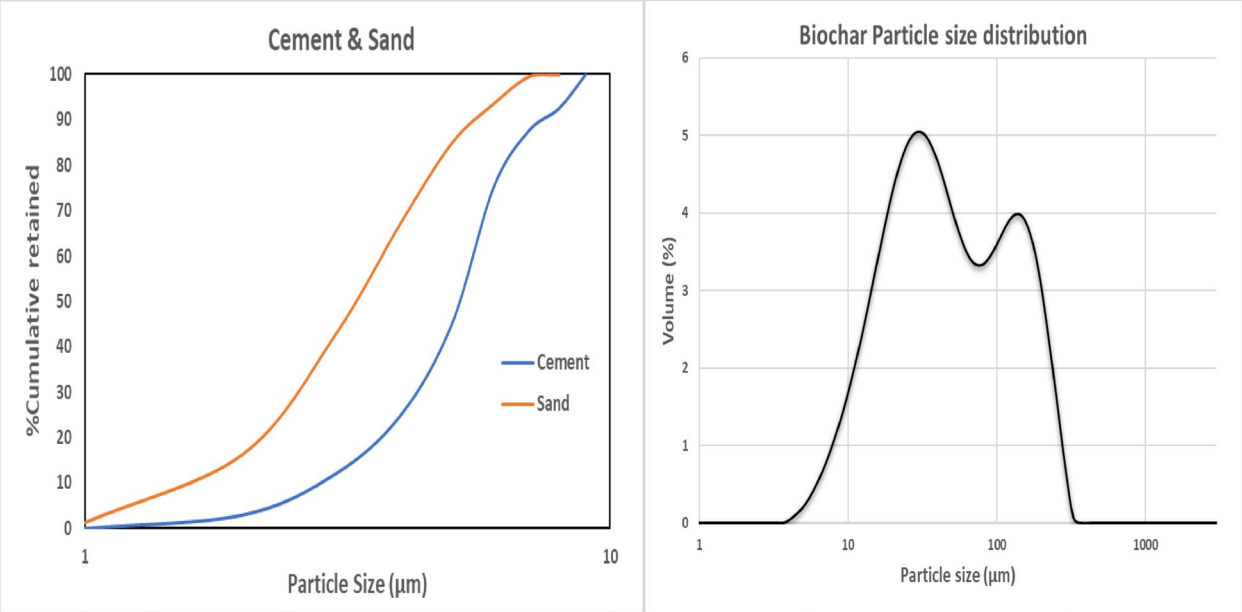

Fig. 1. Particle size distribution of cement, sand and biochar (SA) used in this study.

Oxide (wt%)	Gravel	Sand	PC
Na_2O	0.00	1.61	0.00
MgO	0.98	0.44	0.72
Al_2O_3	9.17	5.00	2.15
SiO_2	46.51	60.50	13.43
P_2O_3	1.70	2.90	0.00
SO_3	0.00	0.14	4.31
ZnO	0.00	0.00	0.18
CuO	0.45	0.47	0.38
Fe_2O_3	5.30	2.97	4.96
MnO_2	0.21	0.19	0.00
Cr_2O_3	0.00	0.00	0.20
Sc_2O_3	0.00	0.00	0.61
K_2O	5.07	2.61	0.50
CaO	30.47	17.83	72.38

Table 1. Distribution of inorganic fractions in cement, sand, and gravel.

proximate analysis of SA along with calorific values are shown in Table 2. Additionally, the ash composition of biochar is presented in Table 3.

X-ray fluorescence (XRF) spectroscopy

The inorganic oxides composition of GU PC, sand and gravel samples are determined using XRF spectrometry and shown in Table 1. The manufacturer of the GP PC, sand and gravel was Quikrete® cement & concrete Products. The physicochemical and ash composition of biochar is given in Tables 2 and 3.

Biochar thermal and functional characterization

Thermal stability of biochar was performed in the presence of nitrogen at a purge flowrate of 60 ml/min. TGA-5000 instrument (Perkin Elmer, USA) was used for thermal analysis of SA with the ceramic crucible and the original weight is taken as a reference. The heating rate was kept constant throughout the analysis and was 20 °C/min. The TGA/DTGA curve of biochar is shown in Fig. 2(a).

The surface functional groups of the biochar were determined using Attenuated total reflectance-Fourier transform Infrared (ATR-FTIR) spectroscopy. The dried SA powder was used for this analysis. The spectrum was observed in the wavenumbers range of 400–650 cm^{-1} with 4 cm^{-1} spectral resolution. The FTIR spectra of SA is shown in Fig. 2(b).

	Value
Ultimate analysis	
Carbon (%)	72.10
Hydrogen (%)	2.17
Nitrogen (%)	0.35
Sulfur (%)	0.16
Oxygen* (%)	25.22
Proximate analysis	
Moisture (%)	2.40
Ash (%)	17.71
Volatile matter (%)	3.18
Calorific value	
Gross calorific value (MJ/kg)	25.66
Net calorific value (MJ/kg)	24.98

Table 2. Physicochemical composition of biochar. *Oxygen content is measured by subtracting carbon, hydrogen, nitrogen, and sulfur from 100.

	SiO_2	Al_2O_3	Fe_2O_3	CaO	MgO	SO_3	K_2O	Na_2O	TiO_2	P_2O_5	MnO_2	SrO	ZnO
Ash (wt%)	34.72	34.74	8.70	6.10	5.34	3.03	1.17	0.32	1.11	1.88	0.26	0.11	0.04

Table 3. Ash composition of biochar.

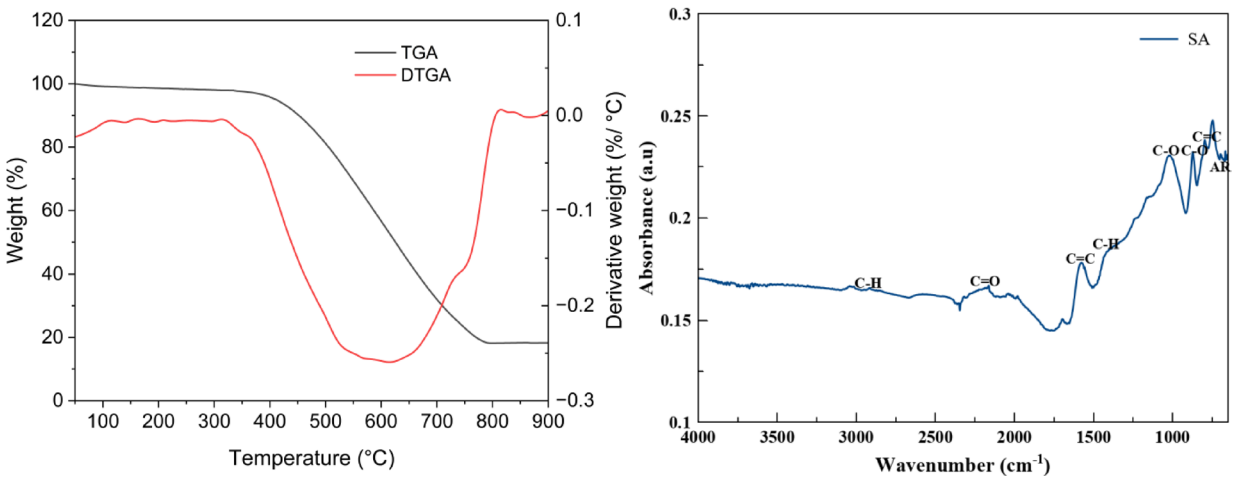

Fig. 2. (**a**) TGA/DTGA curve; (**b**) FTIR spectra of biochar (SA) used in this study (Note: AR—aromatic rings).

Concrete mix and specimen preparation

Fixed designed mixing ratio was used to optimize and study the effect of SA in normal strength concrete. SA was added to the concrete as a partial cement replacement in the weight% of 0–5 (see Table 4). The water-to-binder ratio was kept constant at 0.6 and SA + cement is considered as a binder. The materials were mixed in YARDMAX Portable concrete mixer (4 cu. ft. Drum) having attached dedicated blades for mixing. All the dry materials were first mixed for 2 min and then water was added for further mixing for 2 min. The SA was added to dry mix with the cement powder for proper mixing of the additives. All the samples were casted (Fig. 3) as per ASTM C192/C192M (2016). The cylindrical samples (50 mm x 100 mm), cubes (150 mm x 150 mm x 150 mm), and beam samples (100 mm x 100 mm x 500 mm) were cured as suggested by[54]and tested after predetermined 7, 14, and 28 days of curing for mechanical strength properties as shown in Fig. 4. The slump value is measured immediately after mixing the fresh concrete using the slump cone test and the results are shown in Table 4. The nomenclature of the hybrid samples is given as per the weight% of cement replacement with biochar content, for example, 0.5SA represents 0.5 wt% cement replacement with biochar and similarly for 1SA, 2SA, 2.5SA, 3SA, and 5SA whereas the control sample does not have any biochar. It is noteworthy to mention that there was no other additive like fossil-based superplasticizer water reducer used during the preparation of concrete. The water-holding capacity of biochar reduces the workability of concrete significantly at higher dosage of biochar

	Cement (kg/m^3)	Sand (kg/m^3)	Gravel (kg/m^3)	Water (kg/m^3)	Biochar (kg/m^3)	Slump (mm)
Control	1	2	2	0.6	-	240
0.5% SA	1	2.010	2.010	0.603	0.005	226
1% SA	1	2.020	2.020	0.606	0.010	214
2% SA	1	2.041	2.041	0.612	0.020	198
2.5% SA	1	2.050	2.050	0.615	0.025	186
3% SA	1	2.060	2.060	0.618	0.030	176
5% SA	1	2.100	2.100	0.630	0.050	159

Table 4. Designed mixing ration of biochar-concrete samples with slump value.

Fig. 3. Casted concrete cylinders, cubes, and beam samples for mechanical testing.

which is evident from the slump value measured and mentioned in Table 4. This might result in improper concrete mixing and hence biochar should not be used higher than the acceptable concentration without water-reducing agents.

Experimental tests

Compressive strength

Cylindrical concrete samples of dimensions 50 mm x 100 mm were tested according to ASTM C39 (2016) for compressive strength determination. The capped samples were used for compressive strength measurement and three specimens were tested for each mixing ratio after 7, 14, and 28 days of curing as shown in Fig. 4 and the mean value is considered.

Splitting tensile and flexural strength

The splitting tensile strength of the 50 mm x 100 mm cylindrical specimen was measured as per ASTM C496/C496M (2011) (see Fig. 4). The samples were subjected to splitting tensile test after 7, 14, and 28 days of curing. Similarly, three specimens were tested, and mean values are reported for each mixing design. The beam of the dimensions 100 mm x 100 mm x 500 mm was prepared to measure the flexural strength of the concrete composites. The tests were conducted as per third-Point loading ASTM C78/C78M (2016) standards. Here, all

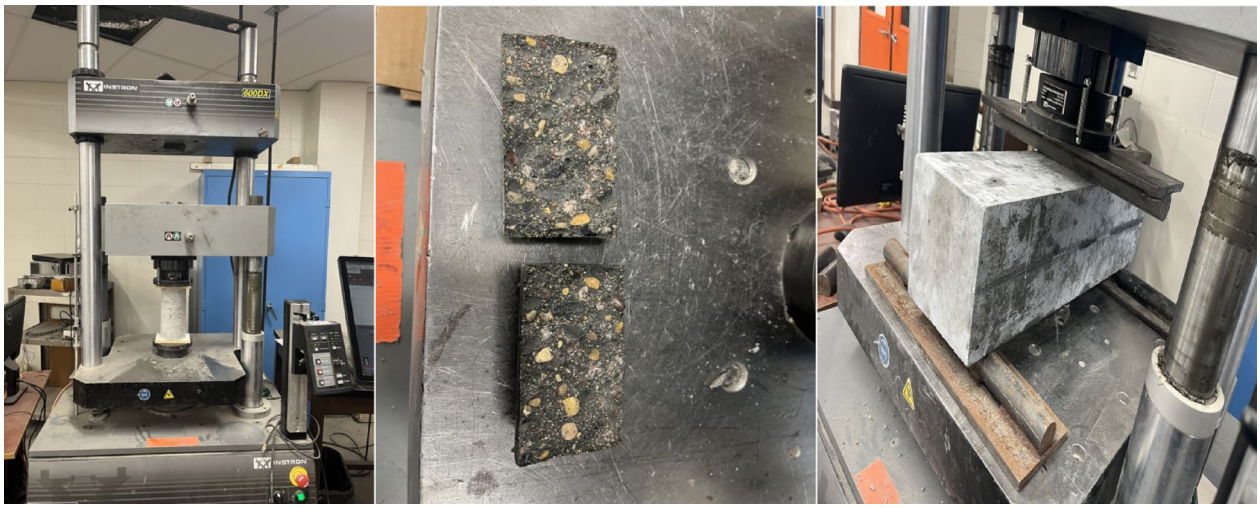

Fig. 4. Compressive, splitting tensile, and flexural bending strength testing of concrete samples using Instron Universal testing machine (UTM).

the tests were done after 28 days of curing and the maximum load at failure was reported for all the mixing ratios as shown in Fig. 4.

Water absorption and density measurement

The water absorption of the samples was measured as suggested by[55]. The cubical samples of $150 \times 150 \times 150$ mm^3 were casted for water absorption experiment and density measurement and tested after 28 days of curing.

X-ray diffraction (XRD) spectroscopy

The hydrated and unhydrated crystalline phases of cured concrete were determined using XRD analysis. The XRD analysis was carried out using Bruker AXS D8 Advance instrument equipped with a graphite monochromator, adjustable slits, and a scintillation detector. The 28 days cured concrete samples were dried in oven for 24 h at 105 °C and then grinded in the hammer mill to fine powder form for the analysis. The spectra were collected at a 2θ angle of 10^o -60^o with the step size of 0.02 at 0.1s per step using Cu-Kα (λ = 1.524 Å) radiation source. The X-ray generator was set at 40 kV voltage and 44 mA current. The XRD of concrete powder is carried out after 28 days of curing.

Synchrotron- based micro-computed tomography (SR-µCT)

Synchrotron-based micro-computed tomography (SR-µCT) allows non-destructive internal 3D imaging at high-resolution of the specimen without damaging it. In this study, we used the BMIT-ID (Biomedical Imaging and Therapy) SR-µCT beamline at the Canadian Light Source (CLS) and is the only facility available in Canada and located in Saskatoon, Saskatchewan[56]. The facility provides much higher contrast than a clinical or conventional CT by using phase contrast imaging (PCI) reconstruction techniques. The system uses an X-ray light source from the beamline, single crystal monochromator, high precision rotation stage, and high-resolution X-ray image detector. The monochromatic X-ray beam was used of energy 85 keV. A total of 2000 projection images, 50 flat images, and 20 dark images with an exposure time of 800 ms. During the CT scanning process, the distance between sample and detector was 0.6 m. The representative concrete cylindrical samples of the dimensions 20 mm x 40 mm were produced for CT experiments. A PCO Edge 5.5 Camera (2160×2560 pixels) coupled with 0.5x AA60 optical lens with an effective pixel size of 13 µm and FOV of 28 mm H x 33 mm W. Camera sensor was cropped to 750 pixels H x 2560 pixels wide. A Yttrium aluminum garnet activated by cerium (YAG: Ce) scintillator of 500 µm thickness was used.

Image processing and further three-dimensional reconstructions were carried out as indicated and described by[57–59]. The data was reconstructed using the TOFU software using the Paganin phase-retrieval method as described by[57,60,61]. Phase Contrast Imaging (PCI) reconstruction parameters of the following were used. SDD: 0.6 m, beam energy: 85 keV, δ/β ratio of 1500 and pixel size: 13 µm. Outlier, large spot, and ring removal filters were used. 32-bit images were converted to 8-bit images by clipping the histograms with minimum and maximum values of 1.741e-15 and 2.878e-14, respectively.

The final image stacks were opened, visualized, filtered, volume rendered, and analyzed in the 3D visualization software Avizo 3D 2020.2 (Thermo Scientific Amira-AvizoSoftware, Thermo Fisher Scientific, Waltham, MA USA). 8-bit histograms were produced in ImageJ software using the bit depth range of grey values, where the darker voxels are air and lighter voxels represent the solid material. The pore size distribution was analyzed by manual selection to investigate each region of interest (ROI), i.e., pores (voids), total porosity (as method described in Fig. 5), pore size distribution (using "label analysis"), and other solid bulk materials from a single slice and plotted against the entire CT histogram and can be seen in Figs. 6, 7, 8 and 9. It's noteworthy to mention that volume editing is done as a part of prescreening of the data to remove the artefacts and better 3D

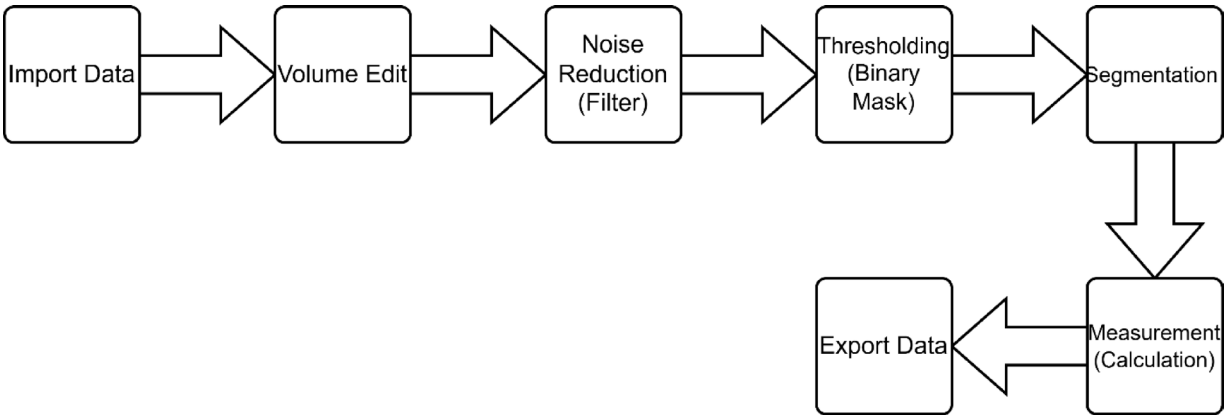

Fig. 5. Porosity analysis procedure used in Avizo 3D software.

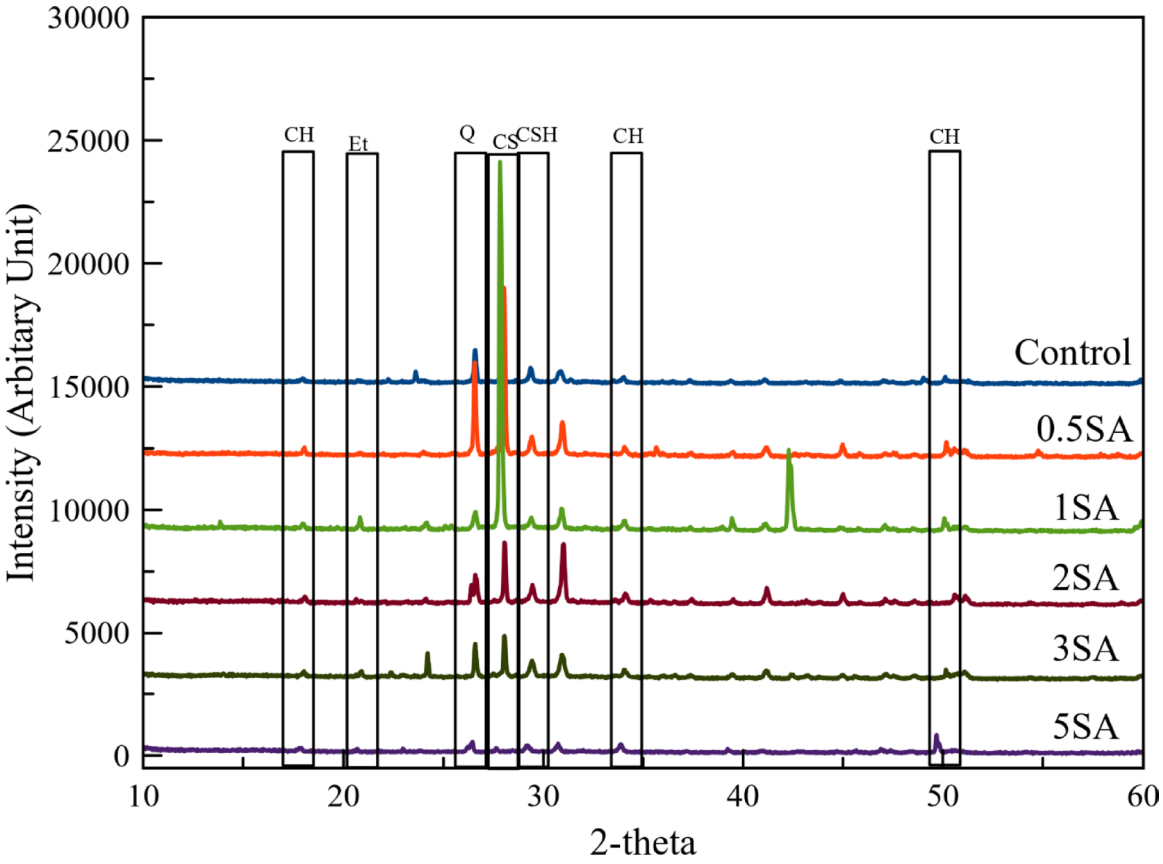

Fig. 6. (**a**) Example of 2D slice of the concrete sample captured using Synchrotron-based CT (Voxel size = 13 µm). (**b**) thresholded image with the porosity using Avizo 3D software. (**c**) binary mask image separating pores and solid material. (**d**) 2D pore view in XY-plane. (**e**) 2D pores in XZ-plane. (**f**) 2D pores in YZ-plane analyzed in Avizo 3D software.

rendering. Moreover, the gaussian filter was used to remove random noises, better image quality and smooth data processing.

Cost analysis

Cement is a fundamental binding material in the construction industry, playing a pivotal role in global infrastructure development. However, the cost of cement production is rising globally due to increasing demand, which not only escalates expenses in the construction and real estate sectors but also impacts national economies. In particular, the current cost of cement production significantly influences the housing market and exacerbates the ongoing housing crisis in Canada. Given these concerns, the incorporation of biochar as a

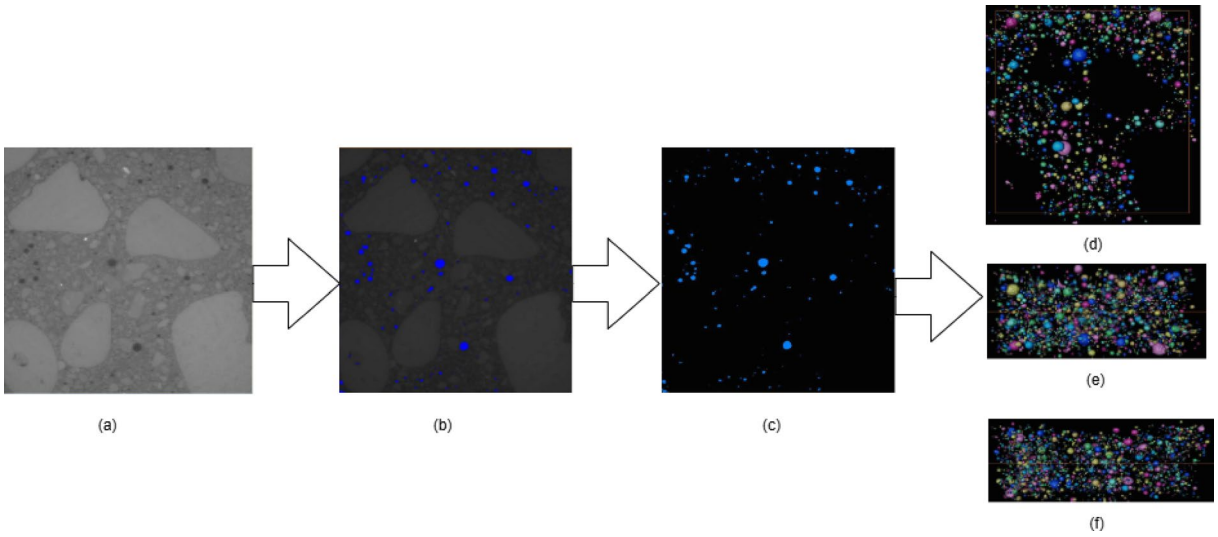

Fig. 7. Pores identified and isolated in 3D view using Avizo 3D software.

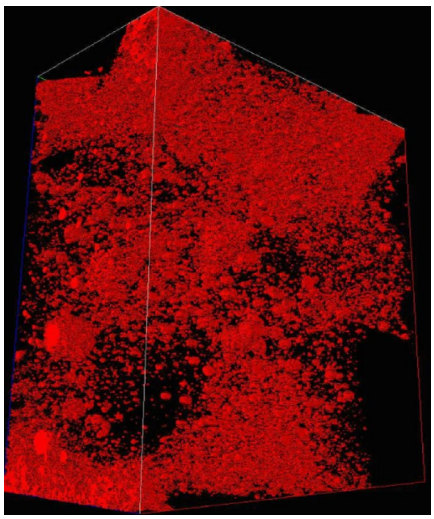

Fig. 8. Histograms of the pore distribution (in volume) for different pore size ranges.

partial replacement for cement presents a potential solution to mitigate or control the overall cost of concrete. This study provides a cost analysis of conventional and hybrid concrete, drawing on previous literature and the current market prices of raw materials used in concrete production as mentioned in Table 5. The cost calculation follows the methodology outlined in Eq. (2) as presented by Thakur et al. (2024). For a literature study and cost comparison of the total ingredients used in making concrete some other biochar was considered at 2 wt% cement replacement with respective biochar for detailed cost analysis as mentioned in Table 5.

$$\text{Total Cost} = \sum_{i=0}^{n} (Ai * Bi) \tag{2}$$

where i = number of ingredients in the mix, n = total number of ingredients in the mix, A_i = the cost of an ingredient i, and B_i = the quantity of ingredient i in kg/m^3. The final cost is multiplied by 1000 to convert the cost into CA$ per tonne/m^3.

Results and discussions

Compressive strength

The results for the compressive strength of cylindrical samples after 7, 14, and 28 days of curing are presented in Fig. 10. The error bars show the variation in the values from its mean value and are represented as standard deviation. At 0.5%, 1% and 2% cement replacement level with biochar showed comparable strength values with

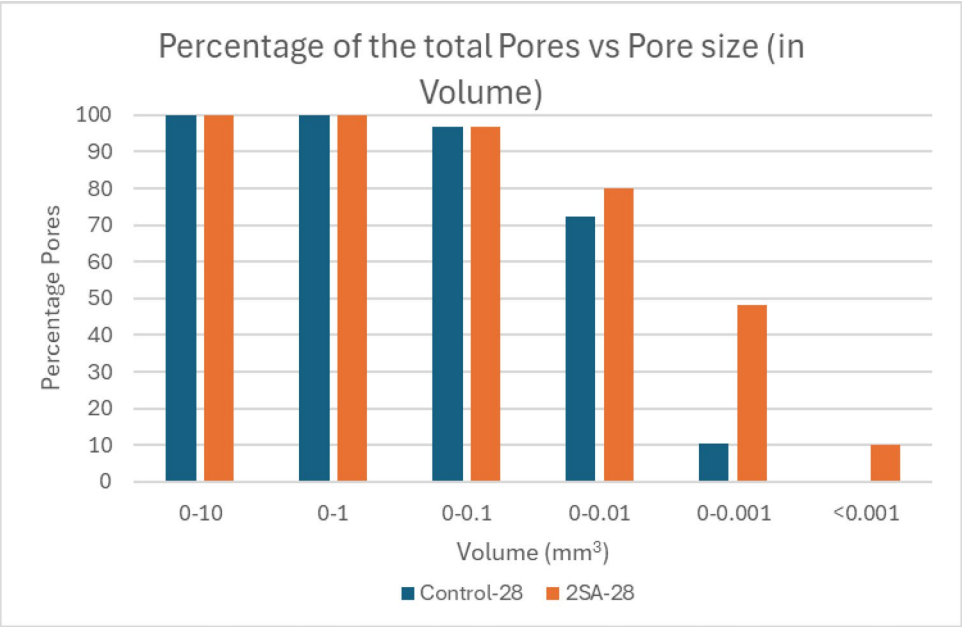

Fig. 9. Histograms of pore volume distribution (in volume) for different ranges of pore size.

Ingredient	Cost (CA $/kg)	References
GU Portland cement (Type 10)	0.53	RONA Garden, Saskatoon, Canada
Sand	0.44	RONA Garden, Saskatoon, Canada
Gravel	0.49	RONA Garden, Saskatoon, Canada
Water	0.00388	City of Saskatoon
Biochar (This study)	0.70	Titan clean energy products, Craik, Saskatchewan, Canada
Water oak wood biochar	1.08	[62]
Coconut shell biochar	1.12	[63]
Oiltea camellia shell biochar	0.94	[64]
Sludge derived biochar	0.98	[65]
Chicken manure biochar	1.82	[66]
Switchgrass biochar	7.68	[62]
Si-modified biochar	2.01	[64]

Table 5. Cost of ingredients used in the study. Conversion rate: CA $1 = 0.72 US$.

respect to control sample after 7 days of curing. That might be because of the similar pozzolanic activity offered by biochar particles with porous structure at the early stages of strength development like cement particles. However, other samples with higher biochar content have shown lower early strength data compared to control samples. After 14 days of curing, the biochar-concrete samples have shown higher compressive strength values (0.60–8.62%) compared to the control samples up to 2% cement replacement. For higher biochar content from 2.5 to 5% reported reduced compressive strength with respect to the concrete without biochar after 14 days of curing. The compressive strength data reflects that the biochar-concrete has a positive impact on the strength properties up to 2.5% cement replacement after 28 days of curing. At optimum biochar addition level, the strength of the hybrid concrete has increased to 32.07 MPa as compared to the control concrete of 26.96 MPa after 28 days of curing. The lower dosages of biochar have shown 0.41% and 6.60% strength enhancement with respect to the concrete without biochar after 28 days of curing. At 2.5% biochar addition the final strength (28 days) of concrete is equivalent to the control sample. At lower dosage, the biochar's water absorption capacity decreases the evaporable free water and therefore reduces capillary pores which subsequently densify the biochar-cement microstructure and boosts up the compressive strength properties of the concrete[67]. The higher dosages of biochar (i.e. 3% and 5%) have reduced strength data related to the controlled concrete after 7, 14, and 28 days of curing. That might be due to the fact of biochar having a porous structure causes increased voids in concrete and hence reduces the overall strength of the concrete. However, up to the optimum dosages of biochar have manifested better pozzolanic reaction that causes strength development from the early stages of the concrete owing to biochar's pore structure refinement properties as mentioned by[1,68]. A literature study[69] on biochar-based mortar suggests that up to 1% replacement of Portland cement with biochar produced from waste

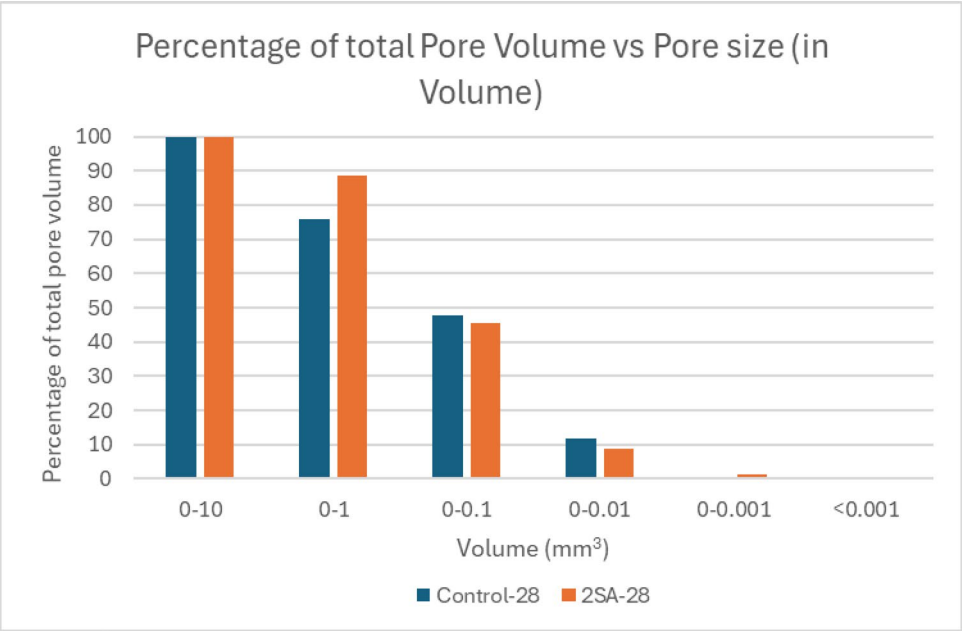

Fig. 10. Compressive strength values for concrete with different cement replacement levels.

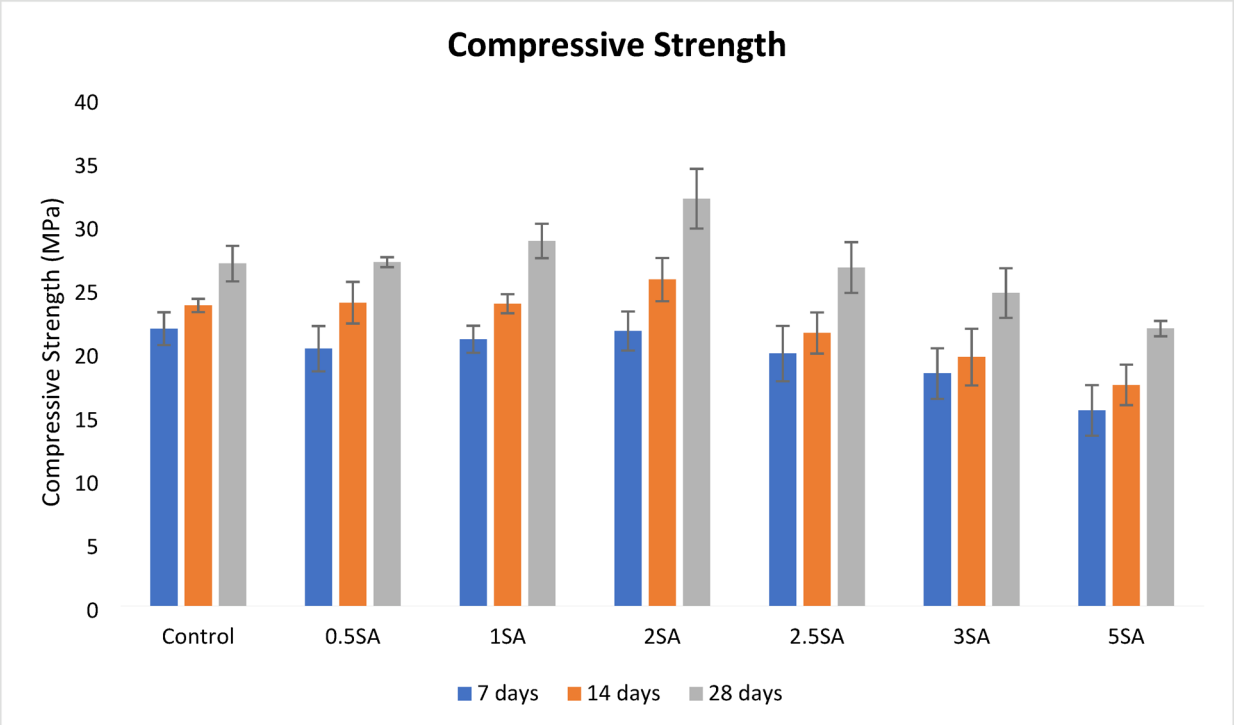

Fig. 11. Splitting tensile strength values for concrete with different biochar content as a cement replacement.

wood tends to increase the compressive strength of the composite, which is also true for concrete composites presented in this study.

Splitting tensile strength and flexural strength

The results of the splitting tensile strength of the control and biochar-concrete are presented in Fig. 11 with the errors bars representing the standard deviation of the data from its mean value. The data presented here is of the concrete after 7, 14, and 28 days of curing. It can be seen that the controlled concrete has slightly improved splitting tensile strength as the curing time enhanced from 7 to 28 days. However, the initial tensile

strength (7 or 14 days) of controlled concrete did not vary significantly compared to the final curing strength (28 days). By addition of biochar the initial splitting tensile strength generally exhibited comparable to lower strength at all the biochar dosages compared to the control concrete which might be because of the porous network properties of biochar-based concrete composites. However, the increased strength has been noticed in the range of 1.07–19.64% by replacing up to 2 wt% of cement. Similar results have been observed after replacing cement with 0.1 wt% rice husk biochar after 28 days of curing[1]. Moreover, they concluded that the biochar affects the splitting tensile strength differently as compared to the compressive strength which sometimes positively contributes to the final splitting tensile properties of biochar. However, at higher replacement levels > 2% has shown lower tensile strength compared to the controlled concrete at any day of curing that might be because the voids created in the concrete generally reduces the overall strength of the composite. Moreover, samples like 2.5SA, 3SA and 5SA exhibited similar patterns in splitting tensile strength as that of the compressive strength, being consistently less than the rest of the samples that can be concluded for their least suitable application in the concrete composites.

The average results are presented in Fig. 12, which shows the maximum load at failure of the concrete specimen after 28 days of curing. The error bars represent the deviation in the maximum load from its average value. The 28-day flexural load data show similar trends as the final compressive strength with and without biochar infused concrete samples. For cement replacement, lower than 2% exhibited comparable to higher maximum load compared to the sample without biochar. The 2SA sample has the highest load at fracture which is about 12% higher than the controlled concrete specimen. Similar > 20% higher strength results by adding 0.1% poultry litter and rice husk biochar, and 1% rice husk biochar to the concrete after 28 days of curing[1]. That can be due to the biochar in concrete acting as a link between the hydrated cement and biochar particles to resist the early fracture of the concrete. The biochar at lower concentration closes the gap of concrete macropores to reduce the overall porosity of the sample and hence increases the bending strength of the cement composites. Tan and co-workers[70]also reviewed and concluded that the cement replacement with 1–3 wt% biochar reduces the permeability by forming dense structure with decreased porosity and enhances the mechanism strength of the cementitious composites. On the other hand, the biochar > 2% showed lower strength data compared to the control concrete that might be attributed to the large number of macro pores accelerating the failure of the specimen when subjected to lower loading.

Water absorption and density

The water absorption pattern with the biochar addition is shown in Fig. 13 for conventional concrete. It can be seen that the 0.5%SA and 2%SA samples have reduced water absorption in concrete than a control sample, where all other samples 1%SA, 2.5%SA, 3%SA, and 5%SA have similar to higher water absorption within 0.33% increment to the control concrete as shown in Fig. 13. The 5%SA sample showed the highest water absorption of 8.27% compared to the control specimen of 7.94%, however the 2%SA sample exhibited least water absorption of 7.44% value. It is important to note that the highest cement replacement level sample 5%SA depicted most water absorption owing to its highest number of permeable voids and also showed least compressive, splitting

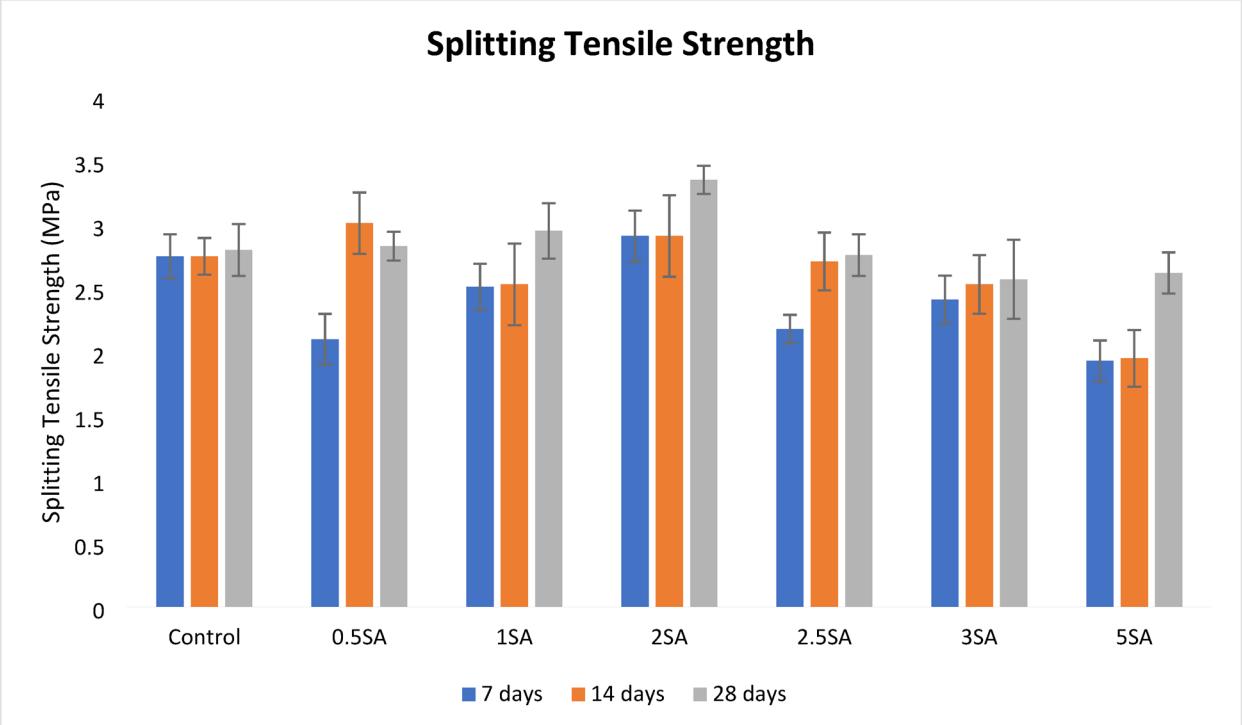

Fig. 12. Maximum load at failure of biochar-concrete composites after 28 days of curing.

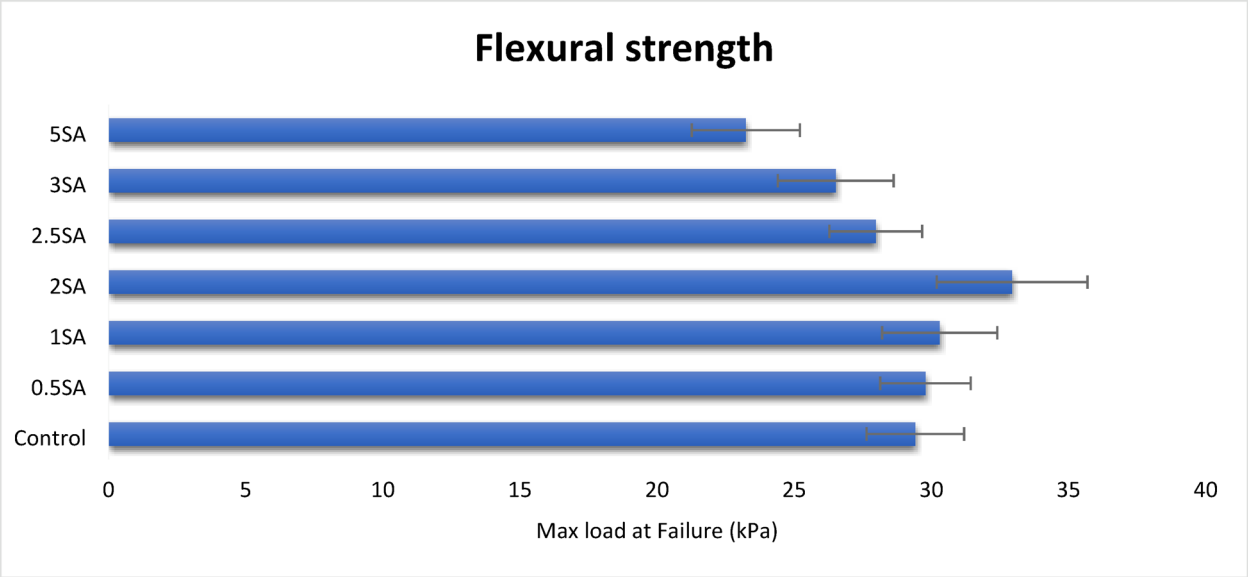

Fig. 13. Water absorption and density of concrete after 28 days of curing.

tensile and flexural strength value compared to the control concrete. Therefore, it can be confirmed that the reduced mechanical strength is attributed to the large water absorption and voids in the concrete specimen which prohibited the formation and dense structure. A similar observation was made by Akhtar and Sarmah[1] after using 0.25% rice husk biochar-concrete which showed the least strength with highest number of permeable voids and hence enhanced water absorption in the sample. In another study, coarser silica fume particles were unable to fill the voids in the concrete leaving behind highly porous concrete, resulting in lower strength concrete with large number of permeable pores[71].

The density values of the concrete samples are also shown in Fig. 13 after 28 days of curing. The strength and durability properties of the concrete are largely affected by the density of the concrete and the supplementary cementitious materials used (i.e. biochar). Generally, the GU Portland cement has higher density than a biochar and the biochar porosity increase with increasing the pyrolytic temperature consequently lowering the density of biochar[72,73]. Here, the density of the biochar increases with the addition of biochar up to 2 wt% cement replacement and then reduces up to 5 wt% replacement than a control concrete sample. The 2%SA sample showed the highest density increment of close to 4% compared to the control specimen, however, the 5%SA sample showed the highest reduced density of 2.25% compared to non-biochar concrete sample. These values are consistent with the water absorption data shown in the same Fig. 13. It can be rationale that a large amount of water absorption is proportional to the large number of voids in the concrete that reduces the overall density of the composite makes it least strong and durable. The smaller particle size and large specific surface area of biochar is beneficial for the faster cement hydration reaction[74]. Moreover, at lower dosage the biochar particles with like finer particle size than the GU Portland cement packs in between the larger cement or fine aggregates forming more dense structure by reducing permeable voids and water absorption and hence increasing the density of concrete specimen. This finding was consistent with rice husk biochar based concrete study at varied concentration which was performed by Akhtar and colleagues[1]and they supported these results by using SEM microscopic analysis. They concluded that higher dosage of biochar negatively impacts the strength and permeability properties of the concrete makes it less compact and weak.

X-ray diffraction analysis (XRD)

The XRD analysis can be used for phase identification of concrete including calcium hydroxide, silica, di- and tri-calcium silicates (C_2S/C_3S), and the calcium-silicate-hydrate (C-S-H) structural phases. The peaks obtained for different concrete samples show varied intensities of hydrated and unhydrated cement phases as shown in Fig. 14. The peaks were obtained for biochar-concrete samples at similar 2θ positions but with different intensities. For example, the control sample showed a relatively lower peak of calcium hydroxide (hydrated lime or portlandite) at around 50.1° compared to 0.5SA, 1SA, and 2SA samples and subsequently exhibited relatively lower intensity peak for C-S-H at 29.4° that offered lower mechanical strength properties for control sample[1,75]. The optimum sample showed the highest peak for calcium-silicate-hydrate products which increases the performance of the concrete and has highest compressive, splitting tensile and flexural strength. It can be concluded that the 2SA sample has the highest peak for the hydrated products which is translated to higher mechanical performance of the concrete. Similar results were found in the case of control sample by[1] when trying to incorporate rice husk, poultry litter, and pulp and paper mill biochar and concluded that biochar can be a viable alternative of cement up to certain dosage, while making concrete for specific applications.

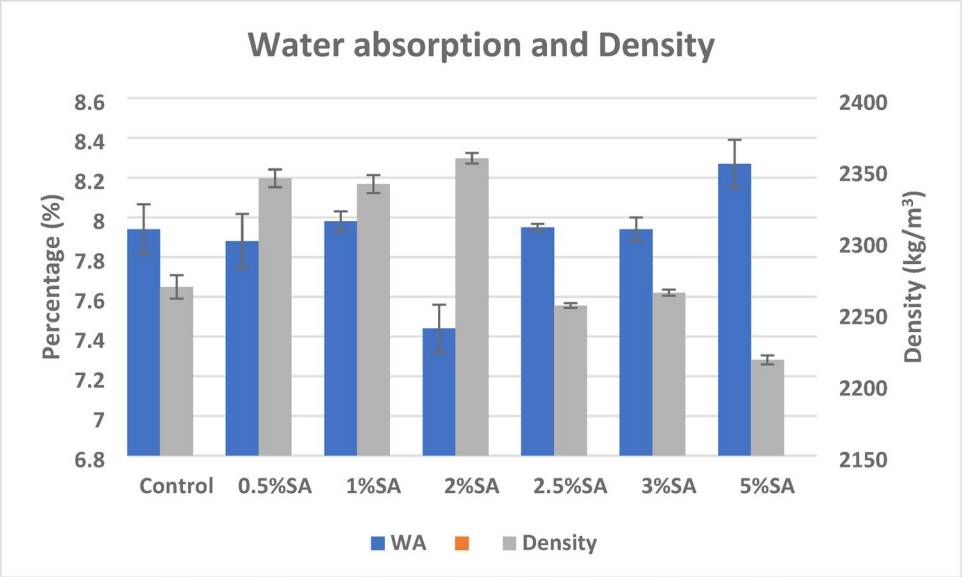

Fig. 14. XRD data of concrete after 28 days of curing (Here, CH, calcium hydroxide; Et, ettringite; Q, quartz; CS, tri/di calcium silicates; CSH, calcium silicate hydrates).

Synchrotron-based computed tomography (SR µ-CT)

The SR-µCT affords researchers a non-destructive approach to investigate internal features, spatial configurations, and overall morphology of specimens, thereby enhancing the understanding of their characteristics and behaviors. This imaging technique employs high-energy X-rays produced by synchrotrons, which interact with varying degrees of X-ray absorption attributable to the distinct components of the sample[76] with a further advantage of employing phase contrast imaging to gain further contrast. The pixel's gray value is directly related to the linear attenuation coefficient of the minerals under examination and is used further to investigate the pores and pore size distribution within the CT image. In the present study, the optimum and control samples after 28 days of curing are investigated using SR-µCT for the non-destructive volumetric microstructural analysis and the acquired images along with the porosity analysis is carried out using Avizo 3D software. The brief analysis of the CT image is shown in Fig. 11 starting from single 2D slice to find pores in different planes and visualize pore distribution in a 3D image in Fig. 6.

Moreover, the histograms of percentage pores and percentage total pore volume for different pore size ranges are shown in Figs. 8 and 9, respectively. The maximum pore size observed for Control and 2SA samples after 28 days of curing were 1.75 mm and 1.37 mm, respectively. It can be seen from the histograms that the majority of the pores in both samples have volumes less than 0.1 mm^3 which was around 97% and 100% of the pores were less than 5 mm^3. The analysis of pores gives an idea of the overall porosity of the specimen, which helps to understand the effect an additive like biochar in the cement matrix. Here using the porosity data measured using Avizo 3D software as a methodology described in Fig. 16, it suggests that 2 wt% biochar incorporation (1.05%) has reduced porosity (by filling pores) compared to the control sample (1.75%), which shows the filling effect of biochar helps in concrete densification, which is also evident from the water absorption data. The histogram analysis shows that the pores are more homogeneously distributed with respect to size in case of biochar (throughout the range), while they are more concentrated on the bigger pore size (mostly > 0.01) in case of a control sample. This fact could be the deciding factor for the overall strength and porosity of the concrete samples, giving optimum biochar sample a higher ultimate strength compared to the control sample. It can also be concluded that the biochar offers the filling effect to reduced porosity and help concrete densification and hence can be used as a sustainable concrete filler to reduce the quantity of cement used.

Cost analysis

The total cost of the ingredients used in the preparation of both the control and biochar-infused concrete samples in this study, as well as data from the literature for a 2 wt% cement replacement with biochar, is presented in Fig. 15. The cost analysis indicates that the control concrete exhibits a lower cost than any of the biochar-modified concretes, primarily due to the relatively low production cost of conventional Portland cement. In contrast, the production cost of biochar remains higher, reflecting current market conditions and the global application of biochar. The thermochemical conversion process employed in biochar production is energy-intensive, further contributing to its higher cost. However, the potential integration of Canada's carbon credit program presents an opportunity to offset the cost of biochar in construction applications which offers CA$ 770/tonne of biochar used which is equivalent to three tonnes of carbon dioxide removal (Supercritical, 2024). This program could significantly reduce the expense of incorporating biochar into construction materials by enabling the sequestration of carbon over extended periods as shown in Fig. 16. The cost of concrete can be reduced by up to 0.66% by supplementing concrete with the biochar, which doesn't seem a lot but looking at

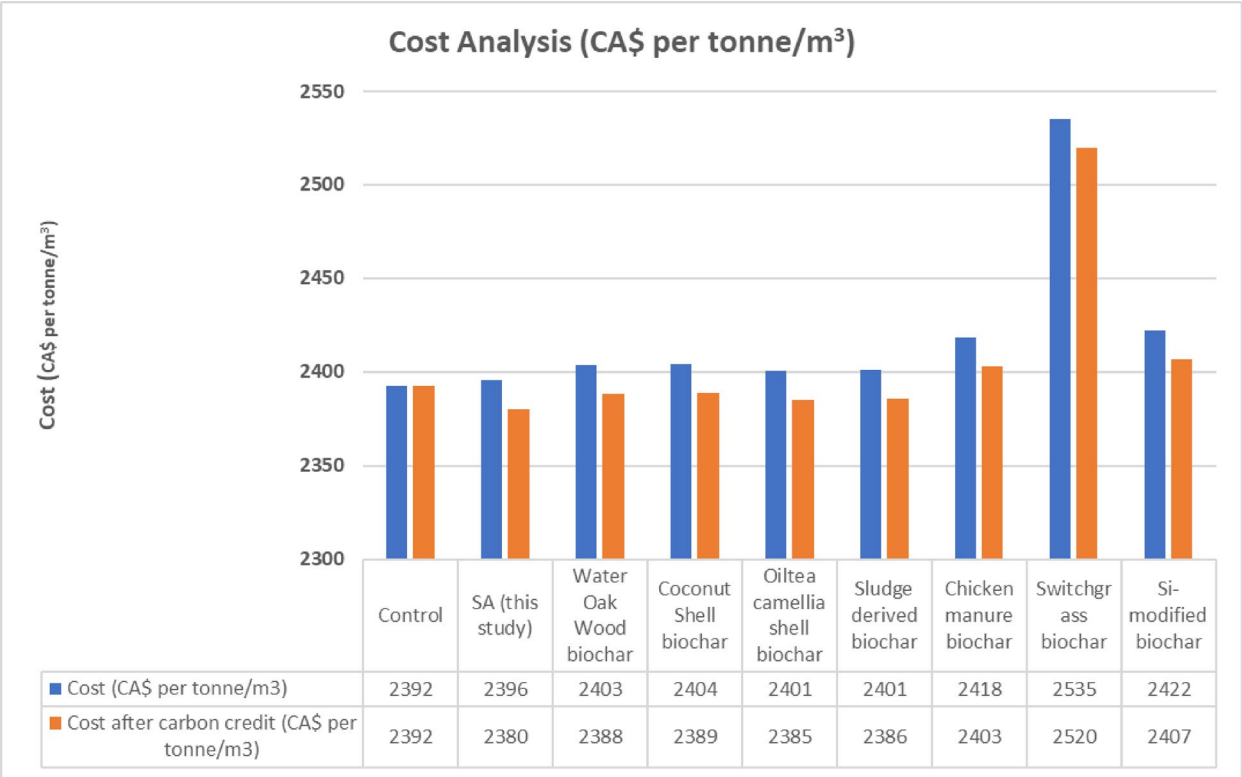

Fig. 15. Total ingredient cost analysis of different concrete.

the billions of tonnes of concrete usage a year can help to save good chunks of money at the end alongside the environmental benefits. Additionally, it holds promises for advancing the green energy sector and mitigating the carbon footprint of the cement industry, as biochar can sequester approximately three tons of carbon dioxide per ton of biochar used. Furthermore, the program not only facilitates cost reduction but also enhances the mechanical properties of concrete, including compressive strength, splitting tensile strength, and flexural strength, through the incorporation of biochar, as highlighted in this study and by Thakur et al.[77]. While higher biochar dosages result in lower costs, they may negatively impact mechanical strength, likely due to an increased number of unfilled pores. Based on the findings of the present study, the 2SA sample is identified as the optimal formulation, as it balances lower cost (through the Carbon Credit Program), reduced water absorption, fewer pores, and enhanced structural strength compared to the control concrete.

Biochar-based concrete: performance prospects and carbon sequestration potential

Conventional concrete production poses a range of challenges pertaining to carbon emissions that need sustainable alternatives to mitigate environmental impacts. This section majorly focuses on the challenges and prospects related to the production and blending of biochar in the concrete to form biochar-concrete.

Biochar can play a crucial role in the sustainability of the construction industry, especially because of its unique characteristics including porous structure, water holding capacity, and low-cost filling properties. As a construction material, biochar can be integrated into the cement, mortar, or concrete to enhance the sustainability and performance characteristics of the cementitious materials. The present study suggests that the mechanical properties including compressive strength, flexural strength, and splitting tensile strength can be improved by incorporating biochar as a bioadditive, while simultaneously reducing the carbon footprints of the construction industry. The principal binder of concrete, which is cement, can be potentially replaced with biochar as a carbon sequestration and eco-friendly alternative without sacrificing the strength properties of concrete. Several studies have indicated the positive effects of biochar-based cement composites and their mechanical and durability properties. Wang et al.[78]investigated the role of biochar and carbon dioxide curing in the sustainable production of magnesia cement-based composites. They found that the incorporation of biochar enhanced the reduced water absorption and compressive strength of the composite. Moreover, CO_2 curing further enhanced the performance of the concrete by improving compressive strength and durability properties, allowing biochar to be used as a sustainable additive to the cement-based composites to produce green construction materials[54]. used the biochar derived from waste wood as an additive for the structural concrete and found that the introduction of biochar enhances the mechanical strength properties of the concrete with reduced carbon footprints. Several researchers[31,79–84] have comprehensively reviewed the alteration of properties by adding biochar in the concrete and discussed the carbon footprints associated with it. The collective data and results suggest the positive outcome for the biochar to be used as a sustainable alternative to the conventional additives in concrete.

In recent years, the potential of biochar-concrete has gained a lot of attention as a possible pathway to reduce the carbon footprints of construction industry. Several researchers including[70,85] dived deeper into the practical performance of biochar-based concrete and its carbon sequestration potential. They found that biochar has a positive impact on reducing carbon emissions and concluded that biochar can be used as an additive in construction materials for the purpose of carbon capture, however these studies lacked in assessing the long-term behavior of biochar-infused concrete composites[86]. explored the biochar-enriched cementitious composites facilitate additional carbon capture from the atmosphere and store it in thermodynamically stable calcite form within the cement matrix[77]. performed the CO2 emission analysis of biochar concrete as a partial cement replacement up to 10 wt%. They found that 10 wt% cement replacement with rice husk biochar can reduce the net CO_2 emissions by 17.8%. It offers a new pathway for rice husk utilization in concrete for environmental conservation and effective solid waste management practices. Moreover, the combination of minerals with biochar as an additive offers a feasible and sustainable solution in offsetting the net CO_2 emissions and aids to develop green carbon-neutral concrete while providing excellent mechanical performance with good CO_2 storage capacity compared to the conventional construction materials.

Conclusions

This study investigates the effect of biochar derived from waste softwood on the enhancement of the mechanical properties of conventional concrete, without the incorporation of polycarboxylate ether-based superplasticizers. The research examines the replacement of cement by varying levels (0–5 wt%) of biochar, which is produced through the pyrolysis of biomass. This approach not only addresses solid waste management but also aims to improve the strength characteristics of construction materials. The results indicate that incorporating up to 2 wt% biochar leads to improved compressive, splitting tensile, and flexural strengths, alongside a reduction in water absorption. At lower concentrations and in the early curing stages, the filler and pozzolanic effects of biochar contribute to the early development of strength, whereas, in later curing stages, the filling effect becomes more dominant, helping to decrease the overall porosity and facilitate the achievement of the concrete's ultimate mechanical properties. This observation is supported by the mechanical strength characterization data.

The key findings of this study are as follows:

1. The inclusion of biochar positively influences the structural properties of concrete.
2. The optimum dosage of 2 wt% biochar as a cement replacement enhances compressive, splitting tensile, and flexural strength at fracture by 18.95%, 19.64%, and 12%, respectively.
3. The 2 wt% biochar replacement exhibits the lowest water absorption, indicating reduced porosity, as confirmed by synchrotron-based CT data.
4. The addition of biochar promotes the formation of more Calcium-Silicate-Hydrate (C-S-H) products, contributing to the highest ultimate strength of the concrete.
5. The cost-effectiveness of biochar-modified concrete could be enhanced, particularly in the context of carbon credit programs.

Furthermore, higher concentrations of biochar result in an increased number of unfilled pores, leading to greater water absorption and a reduction in concrete strength when compared to the control sample, a trend also evident in the mechanical strength and water absorption data. The modification of concrete properties via biochar underscores the importance of further investigation into the large-scale application of solid waste-derived biomass, particularly regarding its long-term durability and mechanical performance. Further research is essential to bridge the gap in developing sustainable green concrete using waste-derived materials, offering potential benefits as a carbon storage solution while producing high-strength concrete with a reduced carbon footprint.

Data availability

The datasets used or analyzed during the present study are available from the corresponding author upon reasonable request.

Received: 25 February 2025; Accepted: 13 June 2025
Published online: 01 July 2025

References

1. Akhtar, A. & Sarmah, A. K. Novel biochar-concrete composites: manufacturing, characterization and evaluation of the mechanical properties. *Sci. Total Environ.* **616–617**, 408–416 (2018).
2. Mindess, S., Young, J. F. & Darwin, D. Concrete Prentice-Hall. *Englewood Cliffs NJ* **481** (1981).
3. Oh, D. Y., Noguchi, T., Kitagaki, R. & Park, W. J. CO_2 emission reduction by reuse of building material waste in the Japanese cement industry. *Renew. Sustain. Energy Rev.* **38**, 796–810 (2014).
4. Yang, K. H., Jung, Y. B., Cho, M. S. & Tae, S. H. Effect of supplementary cementitious materials on reduction of CO2 emissions from concrete. *J. Clean. Prod.* **103**, 774–783 (2015).
5. Oner, A. & Akyuz, S. An experimental study on optimum usage of GGBS for the compressive strength of concrete. *Cem. Concr Compos.* **29**, 505–514 (2007).
6. Saranya, P., Nagarajan, P. & Shashikala, A. P. Eco-friendly GGBS concrete: A state-of-the-art review. in *IOP Conference Series: Materials Science and Engineering* vol. 330 (Institute of Physics Publishing, 2018).
7. Higgins, D. D. Increased sulfate resistance of Ggbs concrete in the presence of carbonate. *Cem. Concr. Compos.* **25**, 913–919 (2003).
8. Ahmad, J. et al. A comprehensive review on the ground granulated blast furnace slag (GGBS) in concrete production. *Sustainability (Switzerland)* **14**, (2022).
9. Khan, M. I. & Siddique, R. Utilization of silica fume in concrete: Review of durability properties. *Resour. Conserv. Recycl.* **57**, 30–35 (2011).

10. Siddique, R. Utilization of silica fume in concrete: Review of hardened properties. *Resourc., Conserv. Recycl.*55 923–932. https://doi.org/10.1016/j.resconrec.2011.06.012 (2011)
11. Mazloom, M., Ramezanianpour, A. A. & Brooks, J. J. Effect of silica fume on mechanical properties of high-strength concrete. *Cem. Concr Compos.* **26**, 347–357 (2004).
12. Sabaa, A., Zeyad, A. M., Mohsen Zeyad, A. & Mostafa Saba, A. Influence of pulverized fly ash on the properties of self-compacting fiber reinforced concrete. *Sci. J. King Faisal Univ. Basic Appl. Sci.* **19** (2018). https://www.researchgate.net/publication/322357824
13. Chindaprasirt, P., Rattanasak, U. & Jaturapitakkul, C. Utilization of fly ash blends from pulverized coal and fluidized bed combustions in geopolymeric materials. *Cem. Concr Compos.* **33**, 55–60 (2011).
14. Liu, M. Self-compacting concrete with different levels of pulverized fuel ash. *Constr. Build. Mater.* **24**, 1245–1252 (2010).
15. Sheng, G., Zhai, J., Li, Q. & Li, F. Utilization of fly ash coming from a CFBC boiler co-firing coal and petroleum coke in Portland cement. *Fuel* **86**, 2625–2631 (2007).
16. Siddique, R. & Klaus, J. Influence of metakaolin on the properties of mortar and concrete: A review. *Appl. Clay Sci.* **43** 392–400. https://doi.org/10.1016/j.clay.2008.11.007 (2009).
17. Zhan, P. et al. Utilization of nano-metakaolin in concrete: A review. *J. Build. Eng.* **30**https://doi.org/10.1016/j.jobe.2020.101259 (2020).
18. Topçu, I. B. & Canbaz, M. Properties of concrete containing waste glass. *Cem. Concr Res.* **34**, 267–274 (2004).
19. Shayan, A. & Xu, A. Value-added utilisation of waste glass in concrete. *Cem. Concr Res.* **34**, 81–89 (2004).
20. Aliabdo, A. A., Elmoaty, A., Aboshama, A. Y. & A. E. M. & Utilization of waste glass powder in the production of cement and concrete. *Constr. Build. Mater.* **124**, 866–877 (2016).
21. Islam, G. M. S., Rahman, M. H. & Kazi, N. Waste glass powder as partial replacement of cement for sustainable concrete practice. *Int. J. Sustain. Built Environ.* **6**, 37–44 (2017).
22. Federico, L. M. & Chidiac, S. E. Waste glass as a supplementary cementitious material in concrete-critical review of treatment methods. *Cem. Concr Compos.* **31**, 606–610 (2009).
23. Shi, C., Meyer, C. & Behnood, A. Utilization of copper slag in cement and concrete. *Resourc., Conserv. Recycl.* **52**, 1115–1120. https://doi.org/10.1016/j.resconrec.2008.06.008 (2008).
24. Moura, W. A., Gonçalves, J. P. & Lima, M. B. Copper slag waste as a supplementary cementing material to concrete. *J. Mater. Sci.* **42**, 2226–2230 (2007).
25. Al-Jabri, K. S., Taha, R. A., Al-Hashmi, A. & Al-Harthy, A. S. Effect of copper slag and cement by-pass dust addition on mechanical properties of concrete. *Constr. Build. Mater.* **20**, 322–331 (2006).
26. Chong, B. W., Othman, R., Ramadhansyah, P. J., Doh, S. I. & Li, X. Properties of concrete with eggshell powder: A review. *Physics Chem. Earth* **120**2020).
27. Yerramala, A. Properties of concrete with eggshell powder as cement replacement point of view properties of concrete with eggshell powder as cement replacement (2014). https://www.researchgate.net/publication/276891886.
28. Tan, Y. Y., Doh, S. I. & Chin, S. C. Eggshell as a partial cement replacement in concrete development. *Magazine Concr. Res.* **70**, 662–670 (2018).
29. Hamada, H. M. et al. The present state of the use of eggshell powder in concrete: A review. *J. Build. Eng.* **32**. https://doi.org/10.1016/j.jobe.2020.101583 (2020).
30. Shu Ing, D., Chin, S. & Siew Choo, C. Eggshell powder: Potential filler in concrete elucidation of lightweight concrete sleeper using oil palm shell and steel slag for railway application view project mechanical properties of high strength concrete that replace cement partly by using fly ash and eggshell powder view project eggshell powder: Potential filler in concrete. (2014). https://www.researchgate.net/publication/283007876
31. Patel, R., Babaei-Ghazvini, A., Dunlop, M. J. & Acharya, B. Biomaterials-based concrete composites: A review on biochar, cellulose and lignin. *Carbon Capture Sci. Technol.* **12**, 100232 (2024).
32. Patel, R., Dhar, P., Babaei-Ghazvini, A., Dafchahi, M. N. & Acharya, B. Transforming lignin into renewable fuels, chemicals, and materials: A review. *Bioresour. Technol. Rep.* **22**, 101463 (2023).
33. Valente, M. & Sibai, A. Rubber/crete: Mechanical properties of scrap to reuse tire-derived rubber in concrete; A review. *J. Appl. Biomater. Funct. Mater.* **17**, 228080001983548 (2019).
34. Siddique, R. & Naik, T. R. Properties of concrete containing scrap-tire rubber - an overview. *Waste Manag.* **24**, 563–569 (2004).
35. Albano, C., Camacho, N., Reyes, J., Feliu, J. L. & Hernández, M. Influence of scrap rubber addition to Portland I concrete composites: Destructive and non-destructive testing. *Compos. Struct.* **71**, 439–446 (2005).
36. Khattak, N. Use of Rubber as Aggregate in Concrete: A Review Seismic Retrofit of Masonry Infilled Concrete Frame Buildings View Project Ishtiaq Alam Water Resources. (2015). https://www.researchgate.net/publication/285682221.
37. Jhatial, A. A., Goh, W. I., Mo, K. H., Sohu, S. & Bhatti, I. A. Green and sustainable concrete–the potential utilization of rice husk ash and egg shells. *Civil Eng. J.* **5**, 74 (2019).
38. Ghayoor, E. A. Effect of partial replacement of cement by mixture of glass powder and silica fume upon concrete strength. *Int. J. Eng. Works Kambohwell Publ. Enterpr.* **4** (2017). http://kwpublisher.com
39. Ahamed, M. S., Ravichandran, P. & Krishnaraja, A. R. IOP Publishing,. Natural fibers in concrete–A review. in *IOP Conference Series: Materials Science and Engineering* vol. 1055 012038 (2021).
40. Balasubramanian, J. C. & Selvan, S. S. Experimental investigation of natural fiber reinforced concrete in construction industry. *Int. Res. J. Eng. Technol.* **2**, 179–182 (2015).
41. Shah, I., Li, J., Yang, S., Zhang, Y. & Anwar, A. Experimental investigation on the mechanical properties of natural fiber reinforced concrete. *J. Renew. Mater.* **10**, 1307 (2022).
42. Geremew, A., De Winne, P., Demissie, T. A. & De Backer, H. Treatment of natural fiber for application in concrete pavement. *Adv. Civ. Eng.* 6667965. (2021).
43. Castillo-Lara, J. F. et al. Mechanical properties of natural fiber reinforced foamed concrete. *Materials* **13**, 3060 (2020).
44. Barnat-Hunek, D., Szymańska-Chargot, M., Jarosz-Hadam, M. & Łagód, G. Effect of cellulose nanofibrils and nanocrystals on physical properties of concrete. *Constr. Build. Mater.* **223**, 1–11 (2019).
45. Aziz, M. A., Zubair, M. & Saleem, M. Development and testing of cellulose nanocrystal-based concrete. *Case Stud. Constr. Materials* **15** (2021).
46. Hisseine, O. A., Wilson, W., Sorelli, L. & Tolnai, B. Nanocellulose for improved concrete performance: A macro-to-micro investigation for disclosing the effects of cellulose filaments on strength of cement systems. *Constr. Build. Mater.* **206**, 84–96 (2019).
47. Wei, R. & Sakai, Y. Improving the properties of botanical concrete based on waste concrete, wood, and kraft lignin powder. *Powder Technol.* **397**, 117024 (2022).
48. Patel, R., Nanda, S. & Dalai, A. K. Conversion of municipal solid waste to biofuels. *Progress. Thermochem. Biorefin.Technol.* 43–61 (2021).
49. Armah, E. K. et al. Biochar: production, application and the future. in *Biochar-Productive Technologies, Properties and Application* (IntechOpen, (2022).
50. Aboughaly, M., Babaei-Ghazvini, A., Dhar, P., Patel, R. & Acharya, B. Enhancing the potential of polymer composites using biochar as a filler: A review. *Polym. (Basel)* **15**, 3981 (2023).
51. Tomczyk, A., Sokołowska, Z. & Boguta, P. Biochar physicochemical properties: Pyrolysis temperature and feedstock kind effects. *Rev. Environ. Sci. Biotechnol.* **19**, 191–215 (2020).
52. Pecha, M. B., Tunstall, L. & Hylton, J. *Biochar as a Building Material: Sequestering Carbon and Strengthening Concrete* (2022).

53. Edeh, I. G., Masek, O. & Fusseis, F. 4D structural changes and pore network model of biomass during pyrolysis. *Sci. Rep.* **13**, 22863 (2023).
54. Sirico, A. et al. Biochar from wood waste as additive for structural concrete. *Constr Build. Mater.* **303** (2021).
55. Sadeghi-Nik, A. et al. The effect of recycled concrete aggregates and metakaolin on the mechanical properties of self-compacting concrete containing nanoparticles. *Iran. J. Sci. Technol. Trans. Civil Eng.* **43**, 503–515 (2019).
56. Gasilov, S. et al. Hard X-ray imaging and tomography at the biomedical imaging and therapy beamlines of Canadian light source. *Synchrotron Radiation*. **31**, 1346–1357 (2024).
57. Stobbs, J. A. et al. Phospholipid self-assembly in cocoa butter provides a crystallizing surface for seeding the form V polymorph in chocolate. *Cryst. Growth Des.* **24**, 2685–2699 (2024).
58. Chen, J., Ghazani, S. M., Stobbs, J. A. & Marangoni, A. G. Tempering of cocoa butter and chocolate using minor lipidic components. *Nat. Commun.* **12**, 5018 (2021).
59. Willick, I. R., Stobbs, J., Karunakaran, C. & Tanino, K. K. Phenotyping plant cellular and tissue level responses to cold with synchrotron-based Fourier-transform infrared spectroscopy and X-ray computed tomography. *Plant Cold Acclimation: Methods Protocols* 141–159 (2020).
60. Faragó, T. et al. A fast, versatile and user-friendly image processing toolkit for computed tomography. *J. Synchrotron Radiat.* **29**, 916–927 (2022). Tofu.
61. Vogelgesang, M. et al. Real-time image-content-based beamline control for smart 4D X-ray imaging. *J. Synchrotron Radiat.* **23**, 1254–1263 (2016).
62. Li, S. & Chen, G. Thermogravimetric, thermochemical, and infrared spectral characterization of feedstocks and Biochar derived at different pyrolysis temperatures. *Waste Manag.* **78**, 198–207 (2018).
63. Alhashimi, H. A. & Aktas, C. B. Life cycle environmental and economic performance of Biochar compared with activated carbon: A meta-analysis. *Resour. Conserv. Recycl.* **118**, 13–26 (2017).
64. Cai, T. et al. Silicate-modified oiltea camellia shell-derived biochar: A novel and cost-effective sorbent for cadmium removal. *J. Clean. Prod.* **281**, 125390 (2021).
65. Cheng, F., Luo, H. & Colosi, L. M. Slow pyrolysis as a platform for negative emissions technology: An integration of machine learning models, life cycle assessment, and economic analysis. *Energy Convers. Manag* **223**, 113258 (2020).
66. Nguyen, M. V. & Lee, B. K. Removal of dimethyl sulfide from aqueous solution using cost-effective modified chicken manure Biochar produced from slow pyrolysis. *Sustainability* **7**, 15057–15072 (2015).
67. Li, H. et al. Elsevier,. Biochar for sustainable construction industry. in *Current developments in biotechnology and bioengineering* 63–95 (2023).
68. Poon, C. S., Lam, L., Kou, S. C., Wong, Y. L. & Wong, R. Rate of pozzolanic reaction of metakaolin in high-performance cement pastes. *Cem. Concr Res.* **31**, 1301–1306 (2001).
69. Pandey, D., Chhimwal, M. & Srivastava, R. K. Engineered Biochar as construction material. in *Engineered Biochar: Fundamentals, Preparation, Characterization and Applications* 303–318 (Springer, 2022).
70. Tan, K., Qin, Y. & Wang, J. Evaluation of the properties and carbon sequestration potential of biochar-modified pervious concrete. *Constr. Build. Mater.* **314**, 125648 (2022).
71. Bozkurt, N. & Yazicioglu, S. Strength and capillary water absorption of lightweight concrete under different curing conditions (2010).
72. Roy, K. et al. Development and characterization of novel Biochar-mortar composite utilizing waste derived pyrolysis Biochar. (2017).
73. Weber, K. & Quicker, P. Properties of biochar. *Fuel* **217**, 240–261 (2018).
74. Thomas, M., Hooton, R. D., Rogers, C. & Fournier, B. 50 Years Old and Still Going Strong. *Concr. Int.* 34, (2012).
75. Maddalena, R., Li, K., Chater, P. A., Michalik, S. & Hamilton, A. Direct synthesis of a solid calcium-silicate-hydrate (CSH). *Constr. Build. Mater.* **223**, 554–565 (2019).
76. Cai, K., Wang, G., Li, W. & Long, W. Numerical simulation of concrete strength based on microstructure and mineral composition analysis using micro-CT and XRD technology. *Constr. Build. Mater.* **432**, 136505 (2024).
77. Thakur, A. et al. Enhancement of concrete performance and sustainability through partial cement replacement with biochar: An experimental study. *Iran.J. Sci. Technol. Trans. Civ. Eng.* 1–21 (2024).
78. Wang, R., Hu, Z., Li, Y., Wang, K. & Zhang, H. Review on the deterioration and approaches to enhance the durability of concrete in the freeze–thaw environment. *Constr. Build. Mater.* **321**, 126371 (2022).
79. Senadheera, S. S. et al. Application of biochar in concrete–a review. *Cem. Concr. Compos.* 105204 (2023).
80. Liu, J. et al. Application potential analysis of biochar as a carbon capture material in cementitious composites: A review. *Constr. Build. Mater.* **350**. https://doi.org/10.1016/j.conbuildmat.2022.128715 (2022).
81. Tan, K. H., Wang, T. Y., Zhou, Z. H. & Qin, Y. H. Biochar as a partial cement replacement material for developing sustainable concrete: An overview. *J. Mater. Civ. Eng.* **33**, 03121001 (2021).
82. Zaid, O., Alsharari, F. & Ahmed, M. Utilization of engineered Biochar as a binder in carbon negative cement-based composites: A review. *Constr. Build. Mater.* **417**, 135246 (2024).
83. Barbhuiya, S., Das, B. B. & Kanavaris, F. Biochar-concrete: A comprehensive review of properties, production and sustainability. *Case Stud. Constr. Mater.* **e02859** (2024).
84. Chen, L. et al. Development of high-strength lightweight concrete by utilizing food waste digestate based biochar aggregate. *Constr. Build. Mater.* **411**, 134142 (2024).
85. Gupta, S., Kua, H. W. & Low, C. Y. Use of Biochar as carbon sequestering additive in cement mortar. *Cem. Concr Compos.* **87**, 110–129 (2018).
86. Mishra, G., Danoglidis, P. A., Shah, S. P. & Konsta-Gdoutos, M. S. Carbon capture and storage potential of biochar-enriched cementitious systems. *Cem. Concr Compos.* **140**, 105078 (2023).

Acknowledgements

The work was supported by MITACS-Accelerate Program [IT29563]- TuniStrong Technologies IncorporatedTM, and Saskatchewan Ministry of Agriculture Research Chair Funds. The author would like to acknowledge Canadian Light Source (CLS), Saskatoon, Saskatchewan, Canada and Saskatchewan Structural Sciences Centre (SSSC), University of Saskatchewan, Canada for providing the analytical facility needed for the research. Part of the research described in this paper was performed at the Canadian Light Source, a national research facility of the University of Saskatchewan, which is supported by the Canada Foundation for Innovation (CFI), the Natural Sciences and Engineering Research Council (NSERC), the National Research Council (NRC), the Canadian Institutes of Health Research (CIHR), the Government of Saskatchewan, and the University of Saskatchewan. CT data handling, processing, and analysis on this paper was partially supported by the grant and contribution-funding program of the National Research Council of Canada. The authors would like to thank Titan Clean Energy Projects for providing biochar samples. The authors also would like to acknowledge Mr. Brennan Pokoyoway, Technician in Civil, Geological and Environmental Engineering, University of Saskatchewan for their help

and support.

Author contributions

R. P.: designed and directed the research and wrote the original manuscript. J.S.: designed the experiments for analytical tools and wrote the manuscript. B.A.: designed and directed the research, provided supervision and wrote the manuscript along with acquiring funding.

Declarations

Competing interests

The authors declare no competing interests.

Additional information

Supplementary Information The online version contains supplementary material available at https://doi.org/10.1038/s41598-025-07210-3.

Correspondence and requests for materials should be addressed to B.A.

Reprints and permissions information is available at www.nature.com/reprints.

Publisher's note Springer Nature remains neutral with regard to jurisdictional claims in published maps and institutional affiliations.